In-flight measurement of the CTI effect on the quantum efficiency of the FI chips at $-110\,$C

Alexey Vikhlinin

March 2, 2000; updated August 2000; updated December 2000

The quantum efficiency of the ACIS FI CCDs decreases at high energies and far from the read-out as a result of the CTI. This memo describes the measurement of this effect using multiple pointings to G21.5–0.9 at the CCD temperature -110C.

G21.5–0.9 was observed in a series of pointing in node 0 of I1, node 2 of I3, and node 2 of S2. Observations were made in July 2000; ACIS temperature was temporarily increased to -110 C. The table lists the observation details and the CTI coefficients (from Brian McNamara).

obsid	chip	node	chipY	CTI/1e-6
1772	i1	0	124	135.6
1773	i1	0	304	135.6
1774	i1	0	484	135.6
1775	i1	0	694	135.6
1776	i1	0	904	135.6
1777	i3	2	304	179.4
1778	i3	2	484	179.4
1779	i3	2	694	179.4
1780	s2	2	304	216.2
1781	s2	2	484	216.2
1782	s2	2	904	216.2

1 Data reduction

I extract the source spectra in PI channels in the *same* regions in sky coordinates. ARFs are calculated using the HRMA effective area file `hrmaD1999-07-22axeffaN0004.fits`, vignetting file `hrmaD1999-07-22vignetN0003.fits`, and the spatially uniform CCD QE from `acisD1997-04-17qeN0002.fits`. The QE curves are individually calibrated for each CCD and presumably are accurate at the readout.

Responce matrices have been generated using the version `_D1999-09-16fef_piN0002.fits` of FEFs for –110C.

For perfectly calibrated CCD QE, HRMA vignetting, and RMFs, these spectra should produce identical fits in XSPEC. If any deviation of the data from the model are observed, this is interpreted as the change of QE or possibly, mirror vignetting.

Since we want to compare the observed spectra of G21.5–0.9 and the Coma cluster in different chip positions, we first need to correct for the CTI-caused gain variations across the CCDs. I used `acis_process_events` with the `acisD1999-09-16gainN0004.fits` gain table to recompute photon energies and PI channels.

The reference spectrum was derived in the 1–9 keV band from S3 pointings (on-axis observations), with CCD QE corrected using QEU files from Norbert Schulz and Sara-anne Taylor.

I tried both power law and broken power law models.

Simple power law fit (Fig. 1) gives the best fit parameters:

```
---------------------------------------------------------------------------
mo = wabs[1]( powerlaw[2] )
Model Fit Model Component  Parameter  Unit     Value
par   par comp
  1    1    1   wabs       nH       10^22      2.310
  2    2    2   powerlaw   PhoIndex             1.844
  3    3    2   powerlaw   norm               1.9903E-02
---------------------------------------------------------------------------
```

There seems to be an excess over the power law model at $E > 7$ keV. This may be due to spatial variations of the power law index (Pat Slane's paper): we have a mixture of steep and flat spectra, and an attempt to fit it with a single power law produces "hard excess". To model this excess, I also tried the broken power law model (Fig. 2):

```
---------------------------------------------------------------------------
mo = wabs[1]( bknpower[2] )
Model Fit Model Component  Parameter  Unit     Value
par   par comp
  1    1    1   wabs       nH       10^22      2.301     +/-  0.2688E-01
  2    2    2   bknpower   PhoIndx1             1.844     +/-  0.1995E-01
  3    3    2   bknpower   BreakE   keV        6.500     frozen
  4    4    2   bknpower   PhoIndx2             1.506     +/-  0.2069
  5    5    2   bknpower   norm               1.9849E-02 +/-  0.5635E-03
---------------------------------------------------------------------------
```

Below I used the broken power law model for the reference spectrum because it seems to fit the data better and to be more physically motivated. All conclusions are the same for the simple power law model.

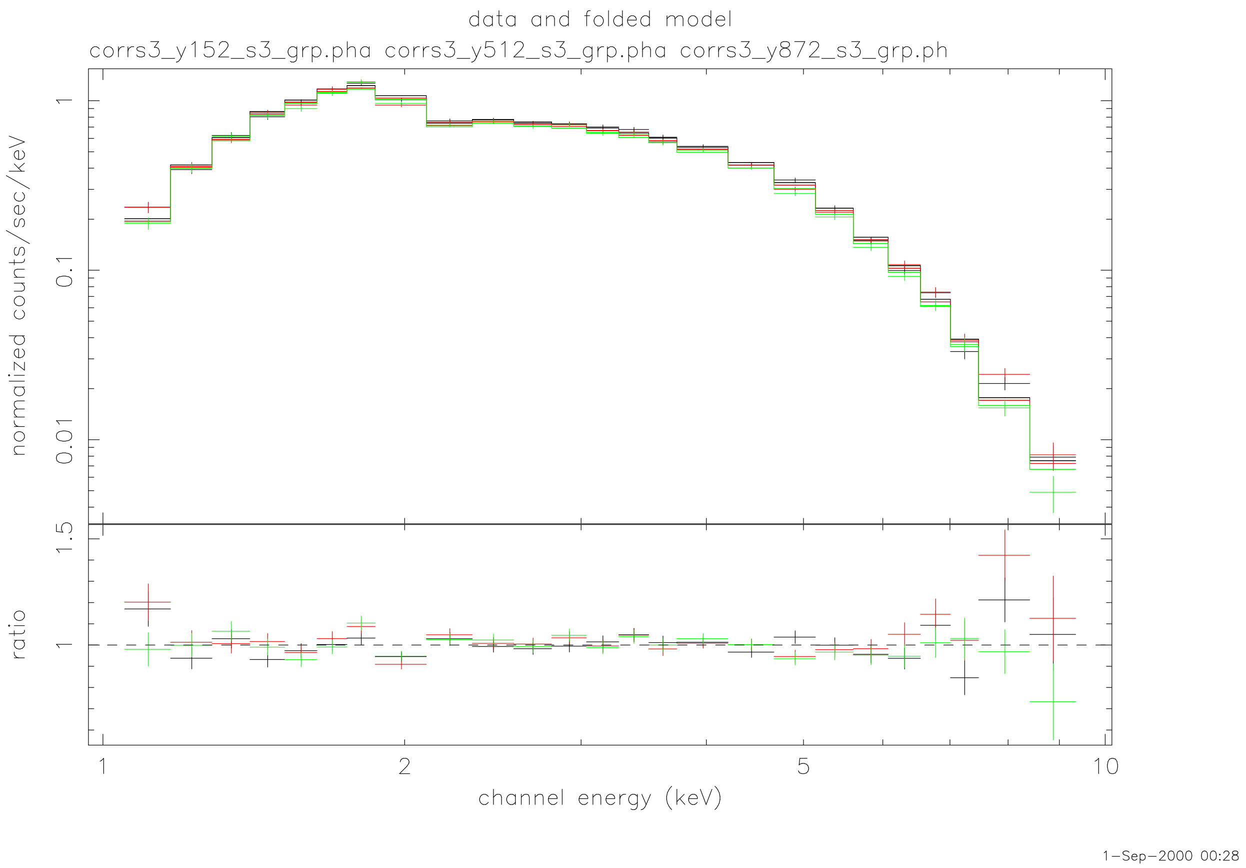

Figure 1: Simple power law fit to G21.5–0.9 in S3.

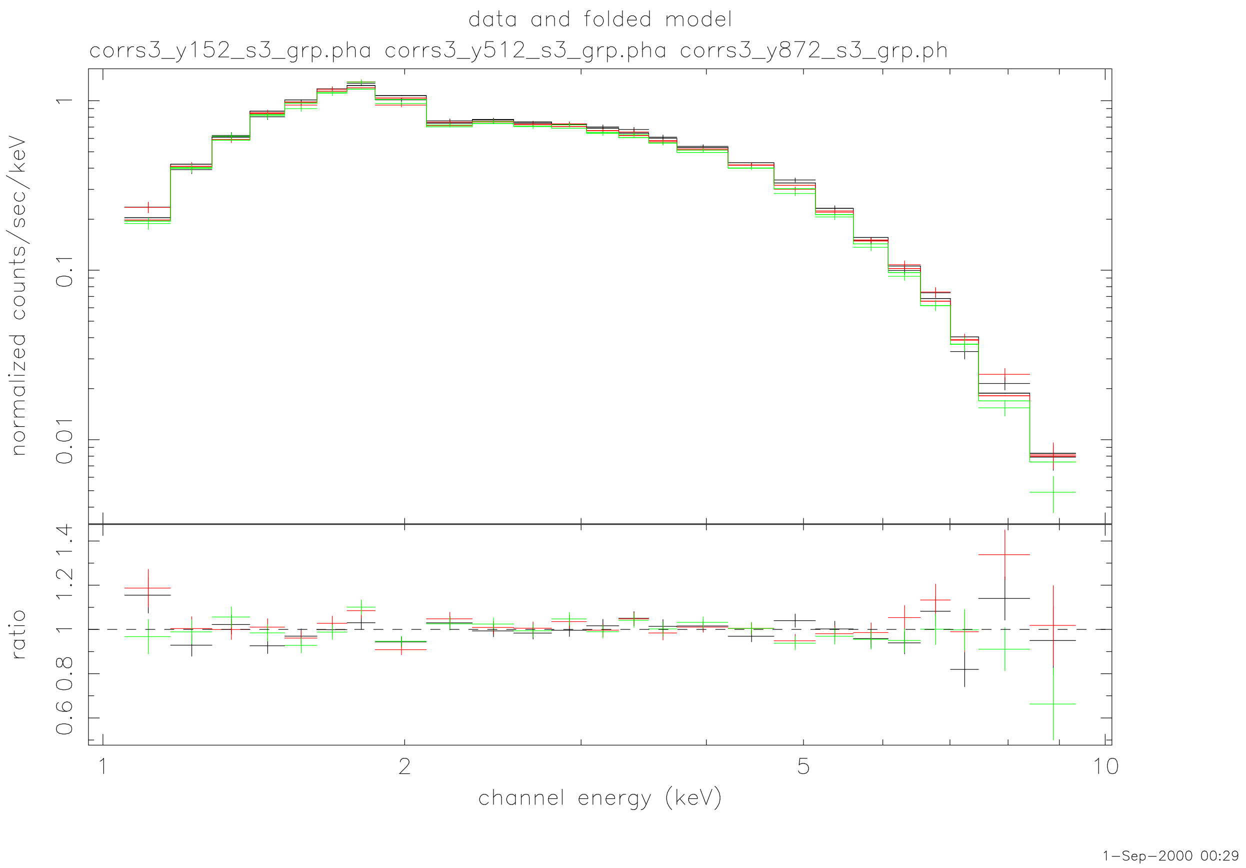

Figure 2: Broken power law fit to G21.5–0.9 in S3.

2 Results

2.1 Energy spectrum of the CTI effect at high energies

Figures 3 and 4 show the ratio of the spectra obtained in FI chips and the S3 model. Here I will concentrate on the data above 2 keV.

The red points in Fig 3 correspond the I1 spectrum at `CHIPY`=124. This region is near the readout and presumably, should not be affected by the CTI. Indeed, the I1/S3 ratio at this `CHIPY` is consistent with 1 within ±5%. Note that the I1,`CHIPY`=124 pointing is $7'$ off-axis, while the S3 data is near the aim point. Therefore, good agreement between the spectra shows that the vignetting calibration is good.

The `CHIPY`=904 spectrum in Fig 3 shows strong deviations from the model at $E \gtrsim 3$ keV. Most likely, this is caused by the QE drop due to CTI. Figure 4 gives more examples. All these spectra show that although the amplitude of the effect varies as a function of `CHIPY` and node,

1. its spectrum is always described by a linear function of $\log E$ above 2.7 keV, and
2. the effect is present only for $E > 2.7$ keV.

I propose that the function

$$\mathrm{QEU}(E, \mathtt{CHIPY}, \mathrm{node}) = \begin{cases} 1 & E < 2.7\text{ keV} \\ 1 - A(\mathtt{CHIPY}, \mathrm{node}) \times \frac{\log(E/2.7)}{\log(6/2.7)} & E > 2.7\text{ keV} \end{cases} \quad (1)$$

is used for the energy dependence of the QEU correction.

2.2 `CHIPY` dependence of the CTI effect at high energies

Figure 5 show the `CHIPY` dependence of the QE drop at 6 keV for July 2000 observations.

1. At large `CHIPY` the effect seems to reach the same amplitude, 0.7, in all nodes, even though the CTI coefficients are very different (see also Fig. 4a).
2. The spatial dependence can be described by a error-function fit

$$A(\mathtt{CHIPY}) = A_0 \times \left(\mathrm{Erf}\left(\frac{\mathtt{CHIPY} - \mathrm{Y}_0}{\Delta}\right) + 1\right) \quad (2)$$

   where the parameters A_0, Y_0, and Δ depend on the node.

3. It is tempting to say that as the CTI coefficient for the node increases, the QE drop starts at progressively smaller `CHIPY`'s. However, the G21.5 data obtained in November-December for other nodes breaks this pattern: there are strong QE drops at `CHIPY`=500 in the nodes with relatively small CTI coefficients. Note that 3 out of 4 of 1999 observations are in the nodes not used for the 2000 observation, so I cannot make any claims about the time dependence of QE.
4. The `CHIPY` dependence derived from the calibration source data also seems to be described by a error-function. However, the cal. source measurements show a significantly smaller amplitude and no dependence on the node's CTI coefficient.

Values of parameters A_0, Y_0, and Δ determine the correction as a function of `CHIPY` in each node. Within the current accuracy of calibration, A_0 should be the same in all chips, while the values of Y_0 and Δ take different values in ACIS-I and S2:

chip	A_0	Y_0	Δ
I0,I1,I2,I3	0.155	540	350
S2	0.155	350	200

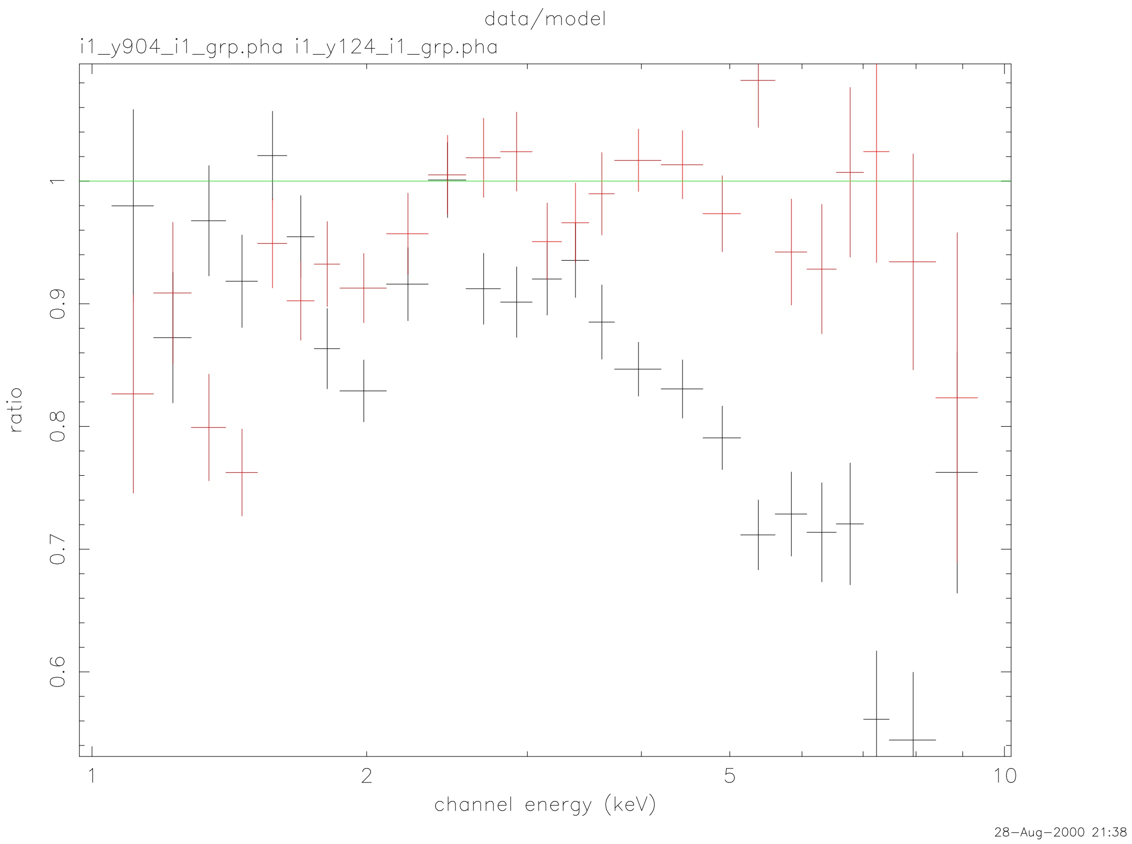

Figure 3: Ratio of the G21.5–0.9 and the reference spectrum in node 0 of I1 at `CHIPY`=124 (red) and 904 (black).

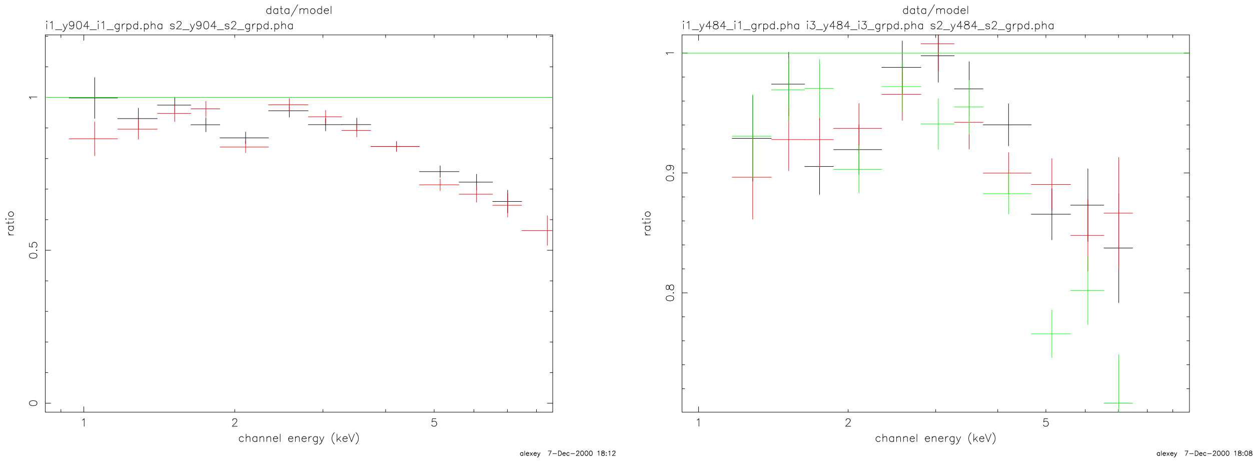

Figure 4: Ratio of the G21.5–0.9 and the reference spectrum. *Left:* I1 and S2 (red and black, respectively) at `CHIPY`=904. *Right:* I1 (black), I3 (red), and S2 (green) at `CHIPY`=484.

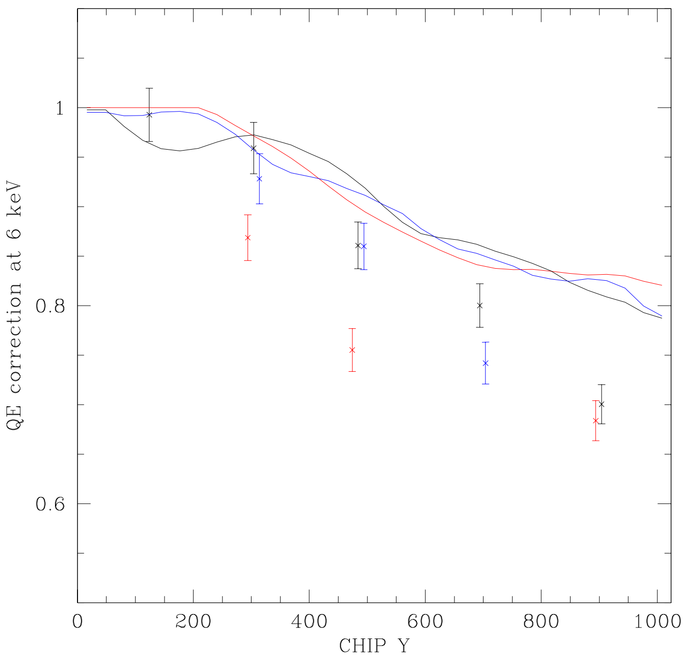

Figure 5: CHIPY dependence of the QE drop at 6 keV for node 0 in I1 (black), node 3 of I3 (blue) and node 2 of S2 (red). Solid lines show the correction derived from the calibration source data (S. Taylor & N. Schulz).

2.3 Problem with cross-calibration between S3 and front-illuminated devices below 2 keV

The spectra in Fig. 4 show that the data in all FI chips at $E < 2$ keV is $\approx 7\%$ below the model fit to the S3 data. This is even more prominent in I1 spectra at CHIPY=124 and 904 (Fig. 3). At $E > 2$ keV, the spectrum at CHIPY=124 is in excellent agreement with the S3 model; this is expected because no degradation is expected at low CHIPY's. However, below 2 keV, this spectrum is $\sim 10\%$ below the model.

Coma cluster observation also shows this problem (Fig 6).

Figure 7 shows that the ratio of 1–1.8 keV fluxes in FI chips and S3 is the same in all nodes, and shows no obvious dependence on the off-axis angle or CHIPY.

The discrepancy at low energies may represent a problem with cross-calibration of the CCD QE between S3 and FI devices. It is also possible that RMF inaccuracies (either BI or FI or both) mimic the QE change at low energies. It is unclear at present which QE (BI or FI) is correct, but spectral fits to the galaxy cluster data suggest that it is the FI chips' QE that needs a correction by a factor of 0.93, if one uses the current (as of Jan 2001) RMFs.

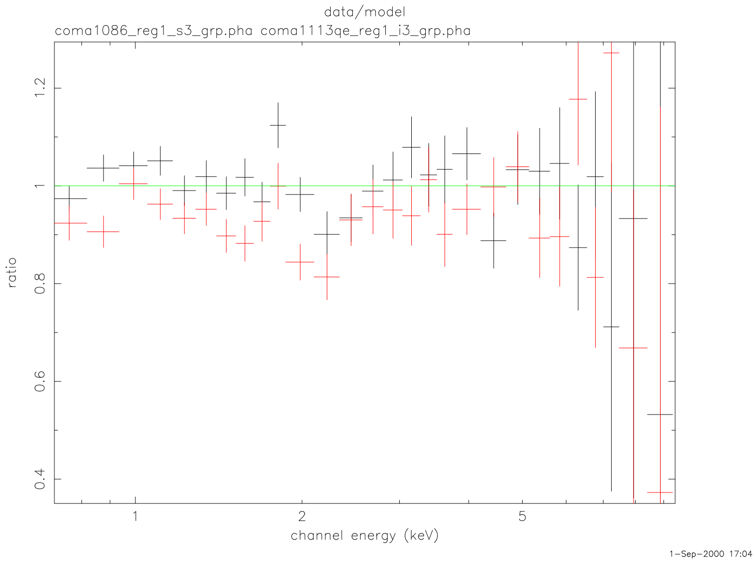

Figure 6: Ratio of the Coma cluster spectra near the aim point in S3 (black) and I3 (red). The model was fitted in S3, and I3 effective area was corrected for the QE drop at high energies.

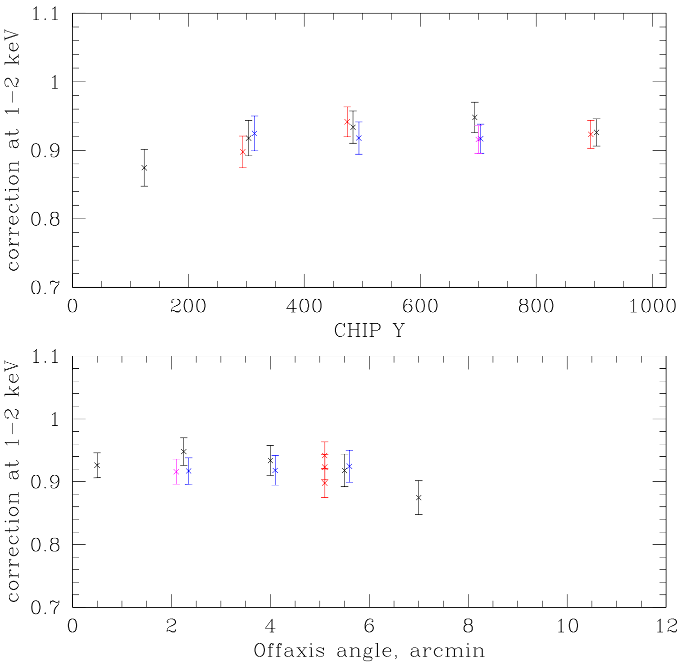

Figure 7: Ratio of the flux 1–1.8 keV flux in S3 and FI devices as a function of off-axis angle and `CHIPY`. Vignetting correction has been applied. Black points are in I1, blue — in I3, and red — S2. The magenta point shows the results for Coma pointings in I3